ROYAL SOCIETY
OF CHEMISTRY

rsc.li/pccp

Journal Name

ARTICLE

A Volumetric and Intra-diffusion Study of Solutions of AlCl₃ in Two Ionic Liquids - [C₂TMEDA][Tf₂N] and [C₄mpyr][Tf₂N]

Kenneth R. Harris, [a*] Noriko Kanai,[b,c] William. S. Price,[b] Allan M. Torres,[b] Scott A. Willis,[d] Theo Rodopoulos,[e] Jean-Pierre Veder[e] and Thomas Rüther.[f]

Intra-diffusion coefficients (D_{Si}) have been measured for the ionic liquid constituent ions and aluminium-containing species in aluminium chloride (AlCl₃) solutions in the ionic liquids 1-(2-dimethyl-aminoethyl)-dimethylethylammonium bis(trifluoromethylsulfonyl)amide ([C₂TMEDA][Tf₂N]) and N-butyl-N-methylpyrrolidinium bis(trifluoromethylsulfonyl)amide ([C₄mpyr][Tf₂N]), to investigate whether spectroscopically detected interactions between the ions and AlCl₃ affect these properties. Such electrolyte solutions are of interest for the electrowinning of aluminium. The temperature, composition and molar volume dependence is investigated. Apparent ($V_{\phi,1}$) and partial molar (V_1) volumes for AlCl₃ have been calculated from solution densities. For [C₂TMEDA][Tf₂N] solutions, $V_{\phi,1}$ increases with increasing solute concentration; for [C₄mpyr][Tf₂N] solutions, it decreases. In pure [C₂TMEDA][Tf₂N], the cation diffuses more quickly than the anion, but this changes as the AlCl₃ concentration increases. In the [C₄mpyr][Tf₂N] solutions, the intra-diffusion coefficient ratio remains equal to that for the pure ionic liquid and the aluminium species diffuses at approximately the same rate as the anion at each composition. The intra-diffusion coefficients can be fitted to the Ertl-Dullien free volume power law by superposing the iso-concentration curves with concentration dependent, but temperature independent, molar volume offsets. This suggests that they are primarily dependent on the molar volume and secondarily on a colligative thermodynamic factor due to dilution by AlCl₃. AlCl₃ complexation by [Tf₂N]⁻ and [C₂TMEDA]⁺, confirmed by ²⁷Al, ¹⁵N and ¹⁹F NMR spectroscopy, seems to play a minor role. Our results indicate that the application of free volume theories might be fruitful in the study of the transport properties of ionic liquid solutions and mixtures.

Introduction

Ionic liquids are promising electrolytes for the electrodeposition of electropositive metals such as aluminium.[1,2] These metals cannot be electrodeposited from aqueous solutions, instead requiring aprotic media such as molten salts or non-aqueous organic solvents. Current aluminium electrodeposition processes are either extremely energy intensive or employ highly volatile and flammable materials, which is not ideal.[3] Low temperature electrodeposition of aluminium from Lewis acidic chloroaluminate ionic liquids is well known[4,5] and more recently it has been demonstrated from several air and water stable ionic liquids containing AlCl₃.[6,7,8,9,10]

In this paper we examine mixtures of aluminium chloride with two ionic liquids (ILs) of interest as electrolyte components in cells used in the investigation of electrowinning of aluminium.[8-10,11] These are 1-(2-dimethyl-aminoethyl)-dimethylethylammonium bis(trifluoromethylsulfonyl)amide, or [C₂TMEDA][Tf₂N],[12] which has an open-chain cation with an N-donor amine group and N-butyl-N-methylpyrrolidinium bis(trifluoromethylsulfonyl)amide, or [C₄mpyr][Tf₂N],[‡,13] where the cation is cyclic and lacks an electron donor centre (Chart 1).

We have previously reported the electrochemical and transport properties of these two ILs,[12,13] in comparison with those of 1-ethyl-1,4-dimethylpiperazinium bis(trifluoromethylsulfonyl)amide, [C₂dmppz][Tf₂N], which also has a cyclic cation, but with a N-donor atom.[12] These three salts have similar molar volumes, but quite different viscosities, conductivities and ion self-diffusion coefficients.[12] There is no ion association in any of these three ionic liquids as shown by their positive cation-cation and anion-anion Laity resistance coefficients (see Appendix).

Here we compare the volumetric (apparent and partial molar volumes, derived from density measurements) and diffusive (solvent ion and aluminium-containing species intra-diffusion coefficients[§,14,15]) properties of aluminium chloride solutions of [C₂TMEDA][Tf₂N] and [C₄mpyr][Tf₂N] as a function of temperature and of composition, to approximately 1 molal

a. *School of Science, The University of New South Wales, PO Box 7916, Canberra BC, ACT 2610, Australia. E-mail: k.harris@adfa.edu.au*
b. *Nanoscale Organisation and Dynamics Group, School of Science, Western Sydney University, Locked Bag 1797, Penrith, NSW 2751, Australia.*
c. *Graduate School of Engineering Science, Yokohama National University, Yokohama, Kanagawa 240- 8501, Japan.*
d. *Nanoscale Organisation and Dynamics Group/Research Infrastructure, Research Services, Office of the Deputy Vice-Chancellor (Research, Enterprise and International), Western Sydney University, Penrith, NSW 2751, Australia*
e. *CSIRO Mineral Resources, Clayton, VIC 3169, Australia*
f. *CSIRO Energy, Clayton, VIC 3169, Australia. . E-mail: thomas.ruether@csiro.au*
† Electronic Supplementary Information (ESI) available: [Tables of density and self-diffusion data and derived quantities; supplementary figures]. See DOI: 10.1039/x0xx00000x
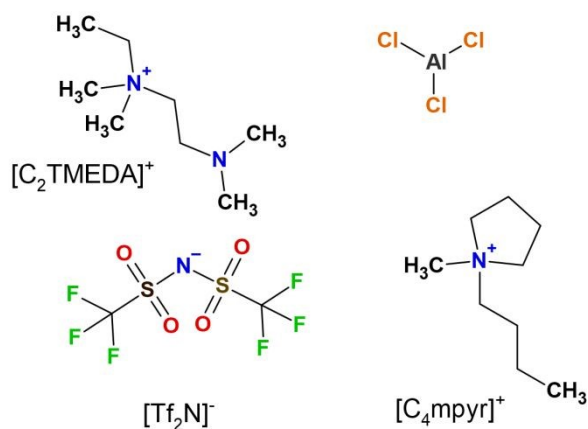
Chart 1. Structure of the component ions of [C₂TMEDA][Tf₂N], [C₄mpyr][Tf₂N] and of AlCl₃.

or mole fraction 0.3, above which the solutions separate into two phases at room temperature or solidify.[9] In addition, ^{27}Al, ^{15}N and ^{19}F NMR spectra are examined.

The [C₂TMEDA][+] ion has a high degree of conformational flexibility. The tertiary amino nitrogen can act as an electron-donor, permitting cation-AlCl₃ complex pair formation, in competition with the [Tf₂N][-] anion. The [C₄mpyr][+] ion, on the other hand, is cyclic, with a quaternary nitrogen in the saturated ring and only the anion can form complexes with AlCl₃ in this case.[8,9] As is well known, the [Tf₂N][-] ion can exist in both *cis* and *trans* conformations, though a high pressure study shows this does not appear to effect self-diffusion in 1-alkyl-3-methylimidazolium ionic liquids:[16] this likely to be generally the case, at least in neat ILs.

The paper is organised into Experimental, Results and Discussion sections.

The Results section reports solution expansivities and apparent molar and partial volumes of AlCl₃ calculated from the solution densities. It also includes consistency checks on the intra-diffusion data using the Litovitz equation for the temperature dependence at each composition and a simple exponential equation for the composition dependence at each temperature employing the molality. These equations are then combined into a general equation for both the temperature and composition dependence.

The Discussion first examines the NMR spectra, correlating these with earlier results. Secondly, differences in the composition dependence of the apparent molar and partial volumes of the two systems are examined. Finally the molar volume dependence of the intra-diffusion coefficients is investigated. The intra-diffusion data are correlated with the solution molar volumes using the free volume power law of Ertl and Dullien, which is found to apply at all compositions.[17,18] This law has been given theoretical justification by Liu[19] using the hard sphere fluid as an example and reference model.

Experimental

Materials.

[C₂TMEDA][Tf₂N] was synthesized and purified as described previously.[12] [C₄mpyr][Tf₂N] and aluminium chloride were obtained from commercial sources. Sample descriptions are given in Table 1. The ionic liquids were dried *in vacuo* for 3 days at 45-50 °C and stored in an argon-filled glove box exposed to lithium chips in a drying tube prior to use. Mixtures were prepared gravimetrically under dry-box conditions (CSIRO, Clayton) at nominal compositions of (0.2, 0.5, 0.7 and 1.0) mol·kg(IL) [-1]. A second batch of [C₂TMEDA][Tf₂N] mixtures used for NMR spin-echo diffusion measurements at WSU had nominal AlCl₃ molalities of (0.16, 0.4, 0.56 and 0.8) mol·kg(IL) [-1].

The solutions were stirred at ambient temperature for two days prior to diffusion and density sample preparation. Water contents for the [C₄mpyr][Tf₂N] solutions were determined by Karl-Fischer coulometry (diaphragm) using standard Honeywell-Fluka Coulomat CG and AG reagents (UNSW). The results for the 0.2, 0.5 and 1.0 mol·kg^{-1} AlCl₃ solutions, following the density measurements, were (670, 1240 and 1050) x 10^{-6} weight fraction respectively. There was insufficient material to permit measurements on the other solutions.

Density Measurements.

An Anton-Paar DMA5000 vibrating tube densimeter (UNSW), with an in-built viscosity correction was used to measure densities, ρ. This correction has been confirmed experimentally.[20] The standard relative uncertainty [$u_r(\rho) = \delta\rho/\rho$, k (coverage factor) = 1][21] based on the substance purities, assuming the main impurity is water, is 0.001. The manufacturer's specification for temperature reproducibility is 1 mK.

Intra-diffusion Measurements.

The intra-diffusion coefficients, D_{si}, i = +, - or Al species, were obtained by two methods.

Steady gradient spin-echo NMR (UNSW), using benzene and water as calibrants, as described in earlier studies,[22,23,24] was employed for cation ([1]H-resonance) and anion (^{19}F resonance) measurements at a fixed frequency of 20 MHz for both sets of solutions at temperatures from 298 to 328 K (depending on the system, ion and concentration) to a maximum of 363 K. Sealed 5 mm NMR tubes were used to contain the samples. A liquid thermostat was employed. Spin-echo heights, E, measured in the time domain, were fitted to the equation[25]

$$E = E_0 \exp\left[-\tfrac{2}{3}\gamma^2 D_{si}\tau^3(g+g_0)^2 \right] \qquad (1)$$

where γ is the appropriate gyromagnetic ratio, τ the 90-180° pulse interval, g the applied magnetic field gradient, which is varied over a range, and g_0 the background gradient. D_{si}, E_0 and g_0 are the fitted coefficients. In most cases, a reported datum is an average of two runs with a range of positive gradients and two with negative gradients, at fixed τ, but some measurements were made with fixed gradients of opposite sign, with τ varied, as a check. There was no evidence of convection at the higher temperatures, with good fits obtained for the Litovitz equation up to 363.15 K (see Discussion). The standard relative uncertainty $u_r(D_{si})$ is estimated at 0.03: for the temperature, the standard uncertainty is $u(T) = 0.01$ K.

Table 1. Sample descriptions

	M/g·	CAS No	source	Manufacturer's purity mol/%	10^6 $w(H_2O)$ [a,b]	10^6 $w(M^+, X^-)$ [c]
[C$_2$TMEDA][Tf$_2$N]	425.417	850256-93-8	Our synthesis[9]	99	57	Li$^+$: < 0.2 Br-: < 100.
[C$_4$mpyr][Tf$_2$N]	422.406	223437-11-4	IoLiTec Lot 10 002 191	99	< 100	X-: < 100
AlCl$_3$	133.336	7446-70-0	Aldrich Lot LKBL8000V	99.99		

[a] Karl Fischer water analysis. [b] w = weight fraction [c] ICP-MS, our analysis.

Intra-diffusion measurements were made for the Al species with the strongest resonance in the [C$_4$mpyr][Tf$_2$N] mixtures [δ(^{27}Al) = 104.8 ppm at 130.32 MHz] using pulsed-gradient stimulated-echo (PGSTE)[26] or double stimulated echo (DSTE)[27] sequences on a Bruker Avance II 500 MHz (11.7 T) wide bore spectrometer and a Diff30 probe over the temperature range 303 - 338 K (Western Sydney University, WSU). This resonance has been assigned previously to the AlCl$_4^-$ anion.[9] Other resonances were found unsuitable for spin-echo intra-diffusion measurements due to signal reduction by short T_2 relaxation times. Additional measurements were made for the cations (averaged over the integrated signals of all the ^{1}H-resonances at 500.13 MHz) from 303 to 338 K as a check on the consistency of the steady gradient and pulsed gradient procedures. The PGSTE and DSTE measurements were performed using half-sine shaped gradient pulses[28,29,30] For the [C$_2$TMEDA][Tf$_2$N] mixtures, cation and anion DSTE measurements were made with a Bruker Avance III HD 600 MHz (14.1 T) wide bore spectrometer (WSU) between 303 and 343 K, again as a check on the steady gradient results. Due to the very short T_2 relaxation times for ^{27}Al in this system, it was only possible to determine an intra-diffusion coefficient for the AlCl$_4^-$ anion at the lowest concentration and highest temperature, 0.16 mol·kg^{-1} and 338 K respectively, with the 500 MHz spectrometer.

The diffusion attenuation equation for the PGSTE sequence[23] with half-sine shaped gradient pulses[28-30] is,

$$E = E_0 \exp\left(-D_S \gamma^2 g^2 \delta^2 \frac{(4\Delta - \delta)}{\pi^2}\right) \quad (2)$$

where Δ is the diffusion time between magnetic field gradient pulses and these have duration δ. The diffusion attenuation equation for the DSTE sequence[27] with half-sine shaped gradient pulses was derived following the procedure outlined for the Stejskal and Tanner[31] pulse sequence with non-rectangular gradients:[25-27]

$$E = E_0 \exp\left(-D_S \gamma^2 g^2 \delta^2 \frac{(4\Delta - 2\delta)}{\pi^2}\right) \quad (3)$$

Note in this case Δ represents the total diffusion time and is the combined separation of the two diffusion gradient pulse pairs (*i.e.*, each stimulated echo has a 'diffusion time' of $\Delta/2$, in the Bruker pulse sequence *dstegp3s1d*).

The original [C$_4$mpyr][Tf$_2$N] samples used for the low frequency measurements were employed here, but a second batch of mixtures was required for the [C$_2$TMEDA][Tf$_2$N] system. DSTE is superior for minimizing the effect of convection,[27] but this was found to be difficult to avoid above 338 K in the present systems as the probe temperature is determined by a flow of temperature regulated air.

The probe was calibrated at 25 °C with the infinite dilution tracer-diffusion coefficient D_T^∞(HDO in D$_2$O)[32,33] using the residual proton signal of HDO in heavy water. The temperature was calibrated using a 100% ethylene glycol standard (Wilmad WGH-07) [or a methanol-d$_4$ standard (WG-R-09-5) for 298 K] and the *calctemp* macro (v. 01.10.2008) in the Bruker Topspin 2.1 software. The standard relative uncertainty $u_r(D_S)$ is estimated at 0.02 for cation (both systems) and anion ({AlCl$_3$ + [C$_4$mpyr][Tf$_2$N]} only) intra-diffusion measurements and 0.05 for AlCl$_3$ measurements (both systems).

NMR Spectra.

^{27}Al NMR spectra for {AlCl$_3$ + [C$_4$mpyr][Tf$_2$N]} mixtures obtained as a function of temperature and composition[8,9] and ^{1}H, ^{13}C and ^{19}F NMR spectral assignments for [C$_2$TMEDA][Tf$_2$N] have been published previously.[13] Further ^{27}Al NMR spectra for the {AlCl$_3$ + [C$_4$mpyr][Tf$_2$N]} mixtures were obtained in this work with both an Agilent VNMRs 400 MHz spectrometer (UNSW) and the Bruker Avance II 500 MHz (11.7 T) spectrometer (pulse-acquire (*zg*) sequence) using a pulse-acquire sequence (WSU). ^{19}F spectra were determined at 376.498 MHz for the same mixtures with a pulse-acquire sequence using a Bruker Avance 400 MHz (9.4 T) spectrometer (WSU). ^{15}N NMR spectra of the neat [C$_4$mpyr][Tf$_2$N] ionic liquid and its 1 molal AlCl$_3$ solution was recorded at 383 K using a Bruker Av400 spectrometer operating at 40.56 MHz whereas that of the neat [C$_2$TMEDA][Tf$_2$N] ionic liquid and its 1 molal AlCl$_3$ solution was recorded at 353 K using a Bruker DRX500 spectrometer operating at 50.70 MHz (CSIRO).

Results

Density.

The densities (ρ_0) of [C$_2$TMEDA][Tf$_2$N] and [C$_4$mpyr][Tf$_2$N] (designated as component 0 in each AlCl$_3$ solution) have been reported previously.[12,13] The experimental densities (ρ) of the AlCl$_3$ solutions are given in Tables S1 and S2 of the ESI.†, with
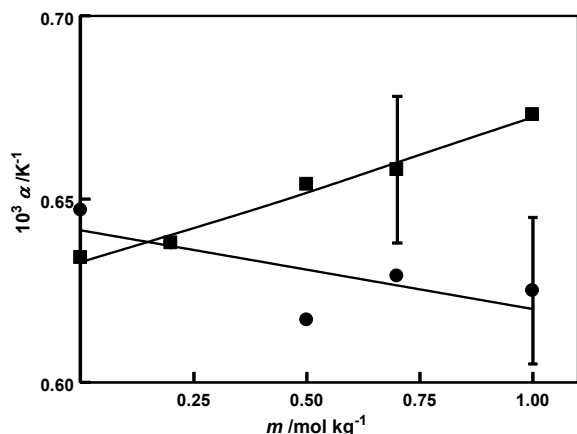
Fig. 1. Mean expansivities (α) of AlCl$_3$ mixtures with [C$_2$TMEDA][Tf$_2$N] (circles) and [C$_4$mpyr][Tf$_2$N] (squares) as a function of molality. The estimated uncertainty is 0.02 10^{-3} K^{-1}.

coefficients for fits to eqn 4 to 6 being given in Table S3 of the ESI.†

$$\rho = a_0 + a_1 T + a_2 T^2 \tag{4}$$

$$\rho = b_0 + b_1 m_1 + b_2 m_1^2 \tag{5}$$

$$\rho = B_0 + B_1 c_1 + B_2 c_1^2 \tag{6}$$

where T is the absolute temperature, and m_1 and c_1 are the molality and molarity (amount concentration) of AlCl$_3$ (component 1). The data sets for the fits included the densities of the pure components.

Expansivities, [$\alpha_p \equiv (\partial V_m / \partial T)_p\,V_m$] $= -(\partial \rho / \partial T)_p / \rho$, where V_m is the molar volume], derived from the fits to eqn 4 are independent of temperature (as for the pure ionic liquids[9,10]): they decrease slightly with increasing AlCl$_3$ content for the [C$_2$TMEDA][Tf$_2$N] mixtures but increase for the [C$_4$mpyr][Tf$_2$N] mixtures (Fig. 1). A negative temperature dependence has been noted previously for [C$_3$mpyr][FSI] (*N*-propyl-*N*-methyl pyrrolidinium bis(fluorosulfonyl)imide) and {Li[FSI] + [C$_3$mpyr][FSI]} mixtures.[34]

The apparent molar volume ($V_{\phi,1}$) represents the change in volume due to the addition of n_1 moles of AlCl$_3$ to n_0 moles of ionic liquid with the assumption that there is no change in the molar volume of the latter, hence the use of the adjective "apparent". $V_{\phi,1}$ is needed for the calculation of thermodynamic volumes but can also be used to analyze solution behaviour directly. Tables S1 and S2 of the ESI† also list apparent molar volumes calculated from the relation

$$V_{\phi,1} \equiv (V - n_0 V_0^0) / n_1 = (M_1 / \rho) - (\rho - \rho_0) / (m_1 \rho \rho_0) \tag{7}$$

where m_1 and M_1 are the molality and molar mass of AlCl$_3$ (component 1) respectively, V is the volume of solution and V_0^0 is the molar volume of the pure ionic liquid. These are shown in Fig. 2. The volumes, which represent the infinitesimal change in solution volume due to the addition of an infinitesimal amount of AlCl$_3$, are defined by

$$V_i \equiv (\partial V / \partial n_i)_{T, p, n_{j \neq 0}}$$

(8)

and can be calculated from fits of $V_{\phi,1}$ to the molarity, c, using the combined expressions of Ellerton *et al.*[35] and of Geffcken:[36]

$$V_{\phi,1} = V_{\phi,1}^\infty + E_1 c \tag{9}$$

$$V_{\phi,1}^\infty = (M_1 - 1000\,B_1) / \rho_0 \tag{10}$$
$$E_1 = -1000\,B_2 / \rho_0 \tag{11}$$

$$V_0 = 1000\,V_{\phi,0}^\infty / [1000 + c_1^2 (\partial V_{\phi,1} / \partial c_1)_T]$$
$$= 1000\,(M_0 / \rho_0) / (1000 + E_1 c_1^2) \tag{12}$$

$$V_1 = V_{\phi,1} + c_1 \left(\frac{1000 - c_1 V_{\phi,1}}{1000 + c_1^2 (\partial V_{\phi,1} / \partial c_1)_T} \right) \left(\frac{\partial V_{\phi,1}}{\partial c_1} \right)_T \tag{13}$$

the coefficients B_1 and B_2 being obtained from the fit to eqn 6: The symbol ∞ denotes infinite dilution. These expressions are more convenient to use than their equivalents based on the molality. Values of the volumes are included in Tables S1 and S2 of the ESI† and shown in Fig. 3.
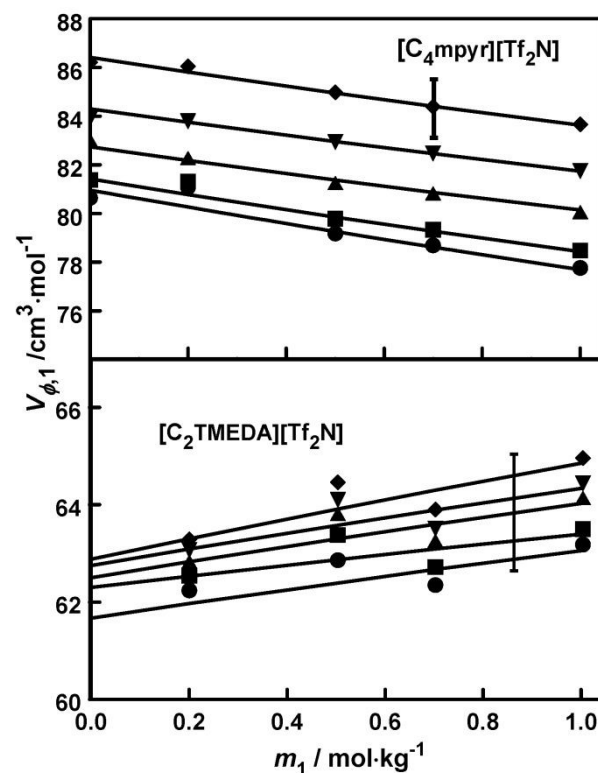

Fig. 2. Apparent molar volumes of AlCl$_3$ ($V_{\phi,1}$) as a function of composition in mixtures with [C$_2$TMEDA][Tf$_2$N] and [C$_4$mpyr][Tf$_2$N] for different isotherms. The data points are calculated directly from the experimental densities; the smoothed curves are derived from the binomial fit of the densities as a function of molarity, c_1, using the Ellerton-Geffcken procedure as described in the text. The error bar is the uncertainty (1.2 cm^3·mol^{-1}, k =1) estimated from this procedure. The deviations of the data points from the smoothed curves in the lower panel may be due to small uncertainties in the compositions. Symbols: ●, 293.15 K; ■, 303.15 K; ▲, 323.15 K; ▼, 343.15 K; ◆, 363.15 K. Intermediate isotherms are omitted for clarity.
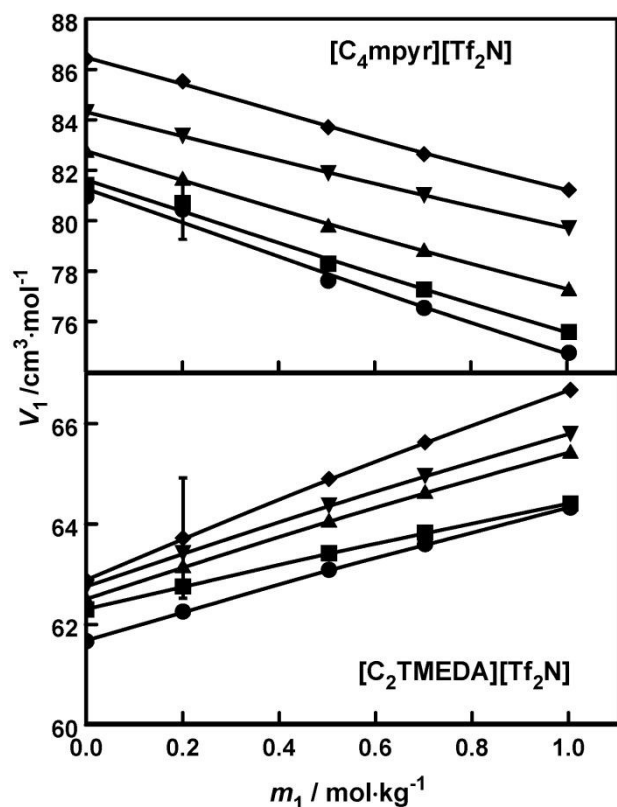
Fig. 3. Partial molar volumes of AlCl$_3$ (V_1) as a function of composition in mixtures with [C$_2$TMEDA][Tf$_2$N] and [C$_4$mpyr][Tf$_2$N] for different isotherms. Note the slightly stronger composition dependence than for $V_{\phi,1}$. The data points are derived from Ellerton-Geffcken procedure as described in the text. The error bars are the uncertainty (1.2 cm$^3 \cdot$mol^{-1}, $\cdot$, k =1) estimated from this procedure. Symbols: as in Fig. 2.

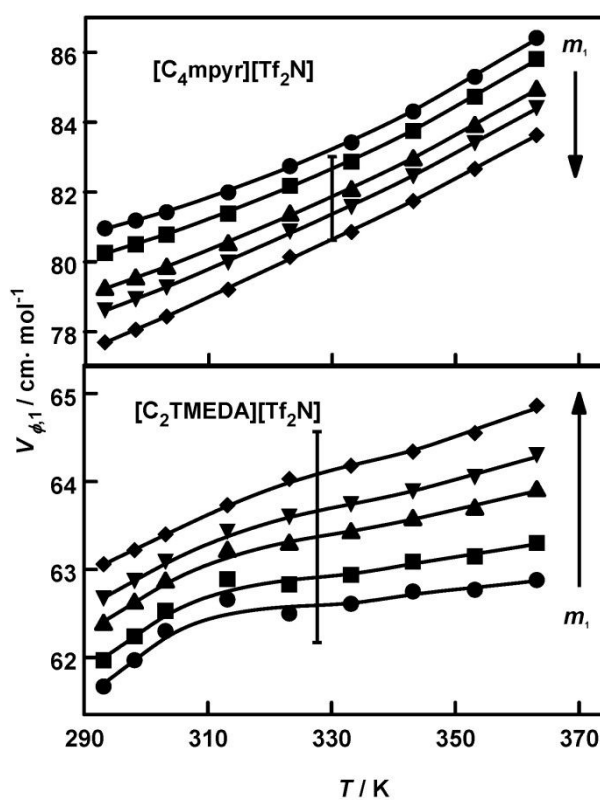**Fig. 4.** Apparent molar volumes of AlCl$_3$ ($V_{\phi,1}$) as a function of temperature in mixtures with [C$_2$TMEDA][Tf$_2$N] and [C$_4$mpyr][Tf$_2$N] for different compositions. The data points are derived from the experimental densities and the lines from the binomial fit of the densities as a function of molarity, c, using the Ellerton-Geffcken procedure as described in the text. Symbols: 0 mol·kg^{-1}, ●; 0.2 mol·kg^{-1}, ■; 0.5 mol·kg^{-1}, ▲; 0.7 mol·kg^{-1}, ▼; 1.0 mol·kg^{-1}, ◆. Note that $V_{\phi,1}$ increases with increasing AlCl$_3$ concentration for mixtures with [C$_2$TMEDA][Tf$_2$N] but deceases for mixtures with [C$_4$mpyr][Tf$_2$N].

Note that both the apparent molar volume ($V_{\phi,1}$) and partial molar volume of AlCl$_3$ (V_1) increase with increasing AlCl$_3$ concentration for [C$_2$TMEDA][Tf$_2$N] solutions and both decrease for [C$_4$mpyr][Tf$_2$N] solutions. The volumes of the solvent ionic liquids (V_0) show the opposite trend in each case, (Table S1 and S2 of the ESI†), though the composition dependences are much weaker than for the solute due to the V_0 values being four to five times larger than V_1. The temperature dependence of $V_{\phi,1}$ is more complex for the [C$_2$TMEDA][Tf$_2$N] mixtures (Fig. 4), with a decrease in slope above about 310 K, which is more pronounced at lower compositions.

Intra-diffusion coefficients.

Values for the cation and anion intra-diffusion coefficients made by the steady gradient technique for both systems are listed in Table S4 of the ESI.† The Table includes intra-diffusion values for pure [C$_4$mpyr][Tf$_2$N] used to supplement those originally reported.[13] There is excellent agreement between the original and new data sets. Values for the cation and aluminium species intra-diffusion coefficients for {AlCl$_3$ + [C$_4$mpyr][Tf$_2$N]} mixtures made by the pulsed gradient technique are listed in Table S5 of the ESI† together with cation and anion intra-diffusion coefficients for {AlCl$_3$ + [C$_2$TMEDA][Tf$_2$N]} mixtures. The pulsed gradient technique allows access to the lower value

D_{Si} found at higher concentrations and lower temperatures where the mixtures are quite viscous. Only one aluminium species intra-diffusion coefficient for the [C$_2$TMEDA][Tf$_2$N] mixture could be measured, at the upper temperature limit of 338 K and the lowest composition (0.16 mol·kg^{-1}), due to the competitive effect of very short T_2 relaxation times.

The intra-diffusion coefficients were fitted to the Litovitz equation at each composition:

$$\ln D_{\text{Si}}(T,m) = \alpha(m) + \beta(m)/T^3 \qquad (14)$$

This two-parameter equation gives good fits for intra-diffusion for most ionic liquids. The coefficients are given in Tables 2 and 3 and fits are shown in Fig. S1 of the ESI.† Fig. 5 shows the composition dependence for both systems (eqn 15) using smoothed values derived from the Litovitz plots.

$$\ln D_{\text{Si}}(T,m) = \varepsilon(T) + \zeta(T)m \qquad (15)$$

The fitted coefficients are listed in Table S6. The slope ζ decreases with increasing temperature in each case.
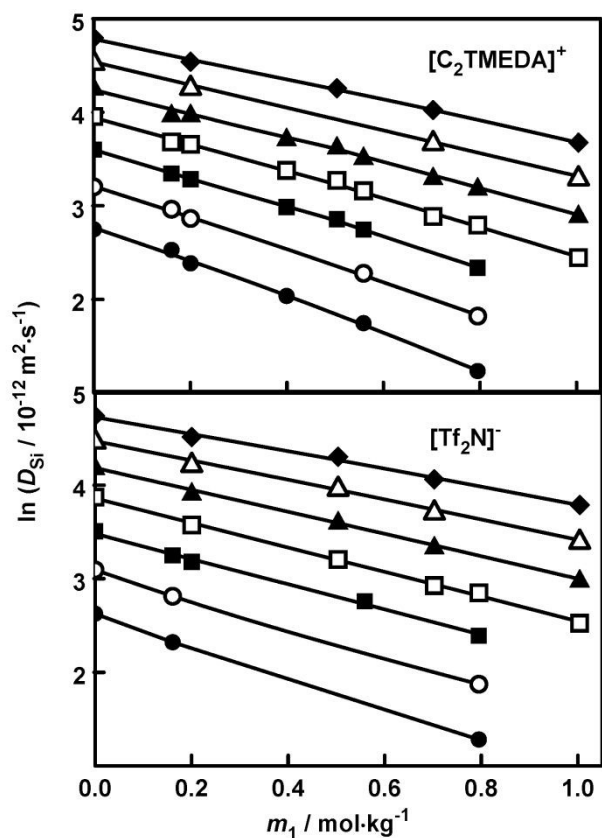
Fig. 5a. Intra-diffusion coefficients for the system {AlCl$_3$ + [C$_2$TMEDA][Tf$_2$N]} as a function of molality m using smoothed values derived from the Litovitz plots at each temperature. Symbols: ●, 303 K; ○, 313 K; ■, 323 K; □, 333 K; ▲, 343 K; △, 353 K; ◆, 363 K. Only a single value could be obtained for the D_s(Al species), at (338 K, 0.1607 mol·kg^{-1}) due to the short Al T_2 relaxation times (see Table S5a).
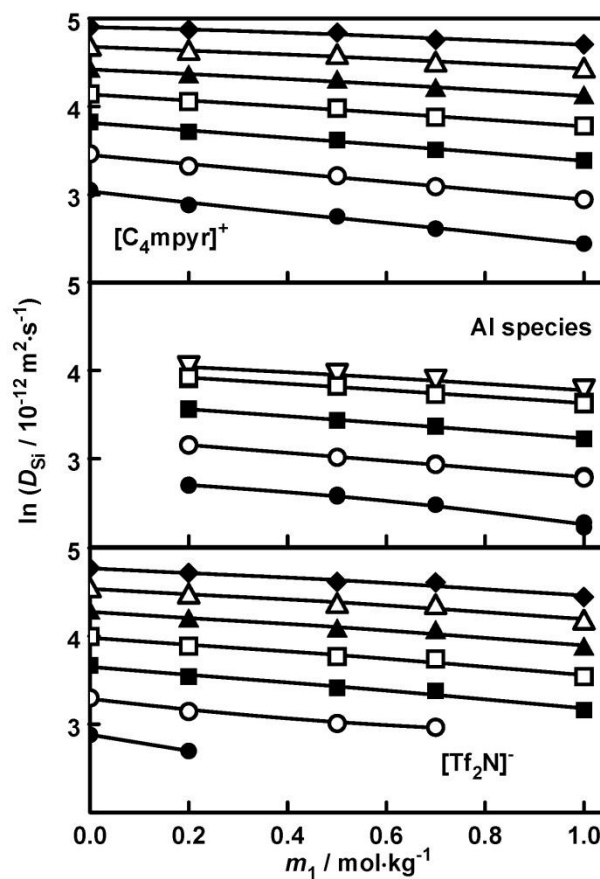
Fig. 5b. Intra-diffusion coefficients for the system {AlCl$_3$ + [C$_4$mpyr][Tf$_2$N]} as a function of molality m using smoothed values derived from the Litovitz plots at each temperature. Symbols: ●, 303 K; ○, 313 K; ■, 323 K; □, 333 K; ▽, 338 K; ▲, 343 K; △, 353 K; ◆, 363 K.

Journal Name

ARTICLE

Table 2. Coefficients of the Litovitz equation, 14, for the intra-diffusion coefficients (D_{si}) at each composition for {$AlCl_3$ + [C_2TMEDA][Tf_2N]}.

m_1 / mol·kg-1	x_1	$10^{12}\,D_{s+}$ /m²·s⁻¹				$10^{12}\,D_{s-}$ /m²·s⁻¹			
		a	$10^{-6}b$/K³	100 u_r [b]	T range / K	a	$10^{-6}b$/K³	100 u_r	T range / K
0 [c]	0	7.6411 ± 0.020	-136.30 ± 0.71	2.4	298-363	7.6896 ± 0.031	-141.09 ± 1.1	4.6	298-363
0.2005	0.0777	7.5376 ± 0.020	-143.51 ± 0.70	2.4	303-363	7.6957 ± 0.036	-152.38 ± 1.4	2.8	318-364
0.5034	0.1745	7.5927 ± 0.046	-159.76 ± 1.8	2.7	323-363	8.0156 ± 0.054	-177.79 ± 2.2	2.8	328-364
0.7027	0.2281	7.8768 ± 0.050	-184.95 ± 2.1	2.6	328-363	7.9043 ± 0.069	-184.03 ± 2.8	2.7	328-363
1.004	0.2970	7.8319 ± 0.052	-199.06 ± 2.2	2.5	328-363	8.0630 ± 0.057	-204.76 ± 2.3	2.3	328-363
0.1607	0.0640	7.2101 ± 0.078	-130.40 ± 2.6	2.6	303 -343	7.636 ± 0.37	-148.1 ± 12	6.1	303-323
0.3994	0.1452	7.480 ± 0.15	-151.62 ± 5.2	4.8	303 -343	-	-	-	-
0.5587	0.1920	7.4806 ± 0.062	-159.77 ± 2.2	2.3	303 -343	7.464 ± 0.22	-158.79 ± 7.8	3.0	323-338
0.7950	0.2527	7.564 ± 0.10	-176.36 ± 3.4	4.8	303 -343	7.6392 ± 0.091	-177.10 ± 2.9	3.7	303-338

[a] m_1 is the $AlCl_3$ molality, x_1 the mole fraction [b] u_r is the standard relative uncertainty of the fit (coverage factor, $k = 1$, so 68% probability that the true value lies in the range of the value given ± one standard deviation; for k =2 the probability is 95% and for k =3 the probability is 99%). [c] From ref. 12.

Table 3. Coefficients of the Litovitz equation, 14, for the intra-diffusion coefficients (D_{si}) at each composition for {$AlCl_3$ + [C_4mpyr][Tf_2N]}

m_1 / mol·kg⁻¹	x_1	$10^{12}\,D_{s+}$ /m²·s⁻¹				$10^{12}\,D_{s-}$ /m²·s⁻¹			
		α	$10^{-6}\beta$/K³	100 u_r [b]	T range / K	α	$10^{-6}\beta$/K³	100 u_r	T range / K
0 [c]	0	7.4779 ± 0.013	-123.30 ± 0.42	1.7	298-363	7.4035 ± 0.025	-126.01 ± 0.83	2.5	298-363
0.1995	0.0777	7.6368 ± 0.021	-132.40 ± 0.72	2.5	298-363	7.5284 ± 0.020	-134.59 ± 0.71	1.7	298-363
0.5003	0.1745	7.7379 ± 0.037	-138.88 ± 1.3	3.4	303-363	7.4831 ± 0.046	-137.34 ± 1.8	2.6	313-363
0.6997	0.2281	7.7411 ± 0.022	-142.80 ± 0.77	1.5	308-363	7.5445 ± 0.059	-140.57 ± 2.2	3.2	308-363
1.004	0.2970	7.8319 ± 0.052	-199.06 ± 2.2	2.5	328-363	8.0630 ± 0.057	-204.76 ± 2.3	2.3	328-363

[a] m_1 is the $AlCl_3$ molality, x_1 the mole fraction [b] u_r is the standard relative uncertainty of the fit ($k = 1$). [c] Additional points from this work combined with those from ref. 13.

Table 4. Coefficients of the concentration modified Litovitz equation, 16, for the intra-diffusion coefficients for {AlCl$_3$ + [C$_2$TMEDA][Tf$_2$N]} and {AlCl$_3$ + [C$_4$mpyr][Tf$_2$N]}.

	{AlCl$_3$ + [C$_2$TMEDA][Tf$_2$N]}		{AlCl$_3$ + [C$_4$mpyr][Tf$_2$N]}		
	$10^{12} D_{s+}$ /m^2·s^{-1}	$10^{12} D_{s-}$ /m^2·s^{-1}	$10^{12} D_{s+}$ /m^2·s^{-1}	$10^{12} D_{s-}$ /m^2·s^{-1}	$10^{12} D_s$(Al species) /m^2·s^{-1}
v	7.6024 ± 0.017	7.7626 ± 0.020	7.5028 ± 0.017	7.4602 ± 0.024	7.4630 ± 0.060
w/ kg·	-	-	0.3864 ± 0.034	-	0.2328 ± 0.089
$10^{-6} y$ / K^3	-134.743 ± 0.59	-144.533 ± 0.73	-124.232 ± 0.56	-128.127 ± 0.83	-129.02 ± 1.0
$10^{-6} z$/ K^3·kg·	-53.949 ± 0.31	-47.331 ± 0.32	-27.69 ± 1.2	-16.01 ± 1.4	-21.75 ± 2.9
100 u_r [a]	3.7	3.9	2.6	3.5	2.0
T range / K	298-363	298-364	293-363	298-363	303-338

[a] u_r is the standard relative uncertainty of the fit (k = 1).
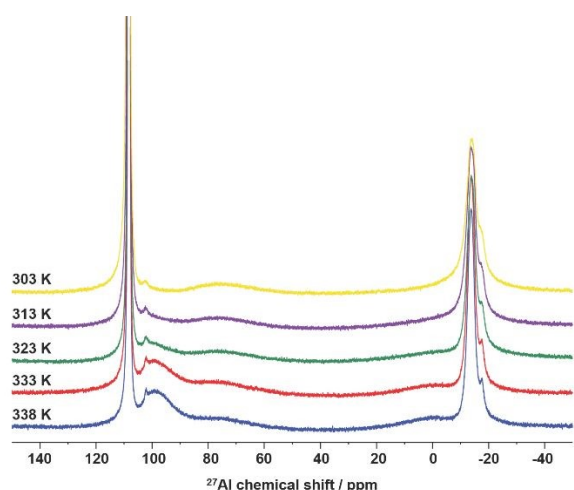
Fig. 6. ^{27}Al spectra acquired at 130.32 MHz using pulse-acquire (*zg*) sequence for the 1 mol·kg^{-1} {AlCl$_3$ + [C$_4$mpyr][Tf$_2$N]} mixture at 303, 313, 323, 333 and 338 K.

More generally, the intra-diffusion coefficients for the mixtures, together with those for pure ionic liquids, were fitted to the concentration modified Litovitz equation, obtained by combining eqn 14 and 15 with the assumption that α and β in eqn 14 have a linear dependence on concentration:

$$D_{si}(T,m) \ = \ exp[v + wm_1 + (y + zm_1)/T^3] \qquad (16)$$

This equation is that used previously to describe lithium–*N*-methyl-*N*-propylpyrrolidinium bis(fluorosulfonyl)imide mixtures, {Li + [C$_3$mpyr][FSI]}.[31] Coefficients are given in Table 4.

Discussion

NMR Spectroscopy.

The ^{27}Al NMR spectrum of molten AlCl$_3$ (m.p.: 485 K), measured between 493 and 533 K, shows a single Lorentzian line at 97.7 ppm.[37] This corresponds to tetrahedrally coordinated Al in

Al$_2$Cl$_6$ dimers where two "AlCl$_4$" tetrahedra share two chlorine atoms along a common edge, a picture supported by ab initio molecular dynamics simulations and quantum-chemical calculations.[38] In the solid state, where Al^{3+} ions are octahedrally coordinated in a chloride lattice, the chemical shift is -1.6 ppm.[37]

In solution, the assignment of spectral peaks is less certain. In a mixture of AlCl$_3$ and 1-ethyl-3-methylimidazolium chloride, 0.52 < *x*(AlCl$_3$) < 0.63, the major peak at 103-105 ppm has also been attributed to tetrahedrally coordinated [AlCl$_4$]$^-$, with a shoulder at 97 ppm attributed to [Al$_2$Cl$_7$]$^-$, again tetrahedrally coordinated.[39] For mixtures of 4-propylpyridine with AlCl$_3$, the main peak at 103 ppm has been assigned to the [AlCl$_4$]$^-$ ion, but a shoulder at 108 ppm was assigned to the tetrahedrally coordinated cationic complex, [(AlCl$_2$)$_4$-PrPyr)$_2$]$^+$, based on supporting infra-red and mass spectroscopic measurements.[40] Zhu et al. have reported higher order chloroaluminate ions at compositions above *x*(AlCl$_3$) = 0.5 in mixtures with 1-methyl-1-propylpyrrolidinium chloride ([C$_3$mpyr]Cl) based on Raman spectroscopic measurements.[41]

As mentioned above, ^{27}Al NMR spectra for {AlCl$_3$ + [C$_4$mpyr][Tf$_2$N]} mixtures obtained as a function of temperature and composition have been published previously.[8,9] Fig. 6 shows spectra at different temperatures obtained with the 1 mol·kg^{-1} solution [*x*(AlCl$_3$) = 0.3] of this work. There are two peaks near 100 to 110 ppm, analogous to those found for AlCl$_3$ in the ionic liquid halides discussed above, and two peaks in the region -10 to -20 ppm. The ^{27}Al NMR and Raman spectroscopy studies of Rocher et al.[8] and Rodopoulos et al.[9] on {AlCl$_3$ + [C$_4$mpyr][Tf$_2$N]} and of Eiden et al.[42] on both {AlCl$_3$ + [C$_4$mpyr][Tf$_2$N]} and {AlCl$_3$ + [EMIM][Tf$_2$N]} support the presence of the symmetric [AlCl$_4$]$^-$ ion as the major peak at around 110 ppm, [AlCl$_3$(Tf$_2$N)]$^-$ as the smaller but broader resonance at around 98 ppm, the strength of which increases with increasing temperature, and Al(Tf$_2$N)$_3$ isomers giving the peaks around -18 ppm.

Fig. 7 is the ^{27}Al spectrum for 0.3994 mol·kg^{-1} {AlCl$_3$ + [C$_2$TMEDA][Tf$_2$N]} at 323 K. It shows the same sharp [AlCl$_4$]$^-$ peak
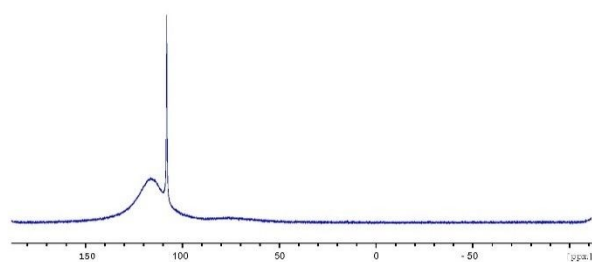
Fig. 7. ^{27}Al spectrum for the 0.3994 mol·kg^{-1} {AlCl$_3$ + [C$_2$TMEDA][Tf$_2$N]} mixture at 323 K.

Table 5. Chemical shifts (δ / ppm) observed in the ^{15}N spectra of the neat [C$_4$mpyr][Tf$_2$N] and [C$_2$TMEDA][Tf$_2$N] ionic liquids and their 1 molal AlCl$_3$ solutions

sample	T /K	[Tf$_2$N]$^-$	quaternary N	tertiary N
[C$_4$mpyr][Tf$_2$N]	383	-240.05	-308.20	-
1 mol·kg^{-1} {AlCl$_3$ + [C$_4$mpyr][Tf$_2$N]}	383	-242.29	-308.10	-
[C$_2$TMEDA][Tf$_2$N]	353	-241.34	-328.24	-363.79
1 mol·kg^{-1} {AlCl$_3$ + [C$_2$TMEDA][Tf$_2$N]}	353	-241.85	-328.41	-360.43
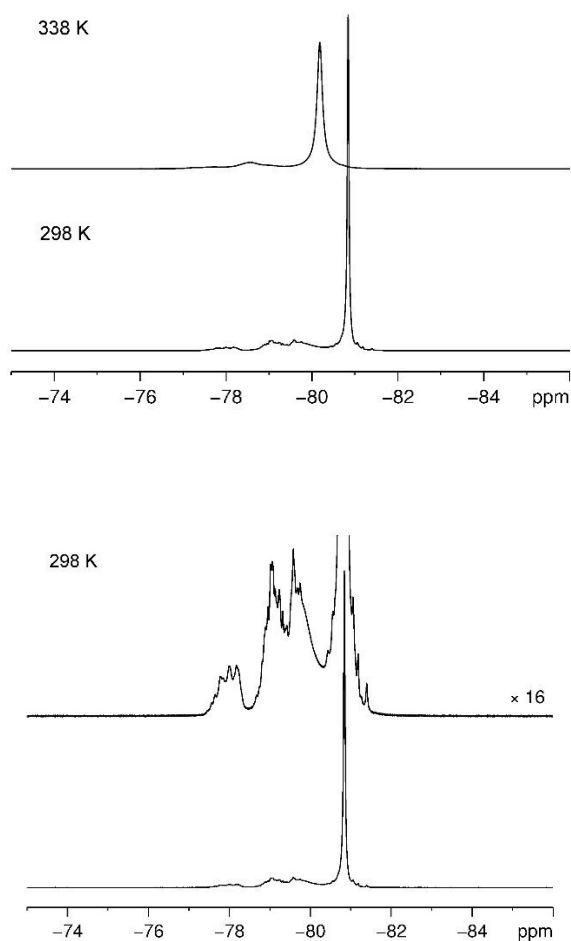
Fig. 8. ^{19}F spectra acquired using pulse-acquire (*zg*) sequence at 376.498 MHz for the 1 mol·kg^{-1} {AlCl$_3$ + [C$_4$mpyr][Tf$_2$N]} mixture. Lower panel: 298 K. Upper panel: comparison of 298 and 328 K peaks; the major peak is broadened and moves downfield slightly (1 ppm) with increasing temperature. Castiglione et al.[44] give a chemical shift of approximately - 80 ppm (graph) for pure [C$_4$mpyr][Tf$_2$N]. For [C$_2$TMEDA][Tf$_2$N], δ = -79.4 ppm:[12] this peak is a singlet in both the neat ionic liquid and its AlCl$_3$ mixtures.

as the {AlCl$_3$ + [C$_4$mpyr][Tf$_2$N]} system, with a broader peak around 115 ppm. However the upfield peaks around - 15 ppm, formed by [Tf$_2$N]$^-$ complexation with Al^{3+} were not detected. This indicates that Al^{3+} complexation by [C$_2$TMEDA][Tf$_2$N] is dominated by the [C$_2$TMEDA]$^+$ cation. Only the [AlCl$_4$]$^-$ peak at 110 ppm had suitable characteristics for intra-diffusion measurements, in both sets of mixtures.

^{15}N spectra of [C$_4$mpyr][Tf$_2$N] and [C$_2$TMEDA][Tf$_2$N] and their respective 1 molal AlCl$_3$ solutions are compared in Table 5. In both AlCl$_3$ mixtures the chemical shifts of the cation quaternary nitrogen are essentially unchanged, relative to the neat ionic liquid, as is to be expected, as no coordination to this nitrogen can occur.

There is a downfield shift of the [C$_2$TMEDA]$^+$ cation tertiary nitrogen peak, relative to the neat ionic liquid, suggesting its coordination to Al^{3+}. This is supported by the presence of the broad peak in the ^{27}Al spectrum at around 115 ppm (Fig. 7) which does not appear in the spectrum of the {AlCl$_3$ +[C$_4$mpyr][Tf$_2$N]} mixture (Fig. 6). [C$_2$TMEDA]$^+$ appears to be a stronger ligand than the [Tf$_2$N]$^-$ anion, where the negative charge is delocalised.[43]

In [C$_4$mpyr][Tf$_2$N] there is an upfield shift in the nitrogen peak for the [Tf$_2$N]$^-$ anion upon addition of AlCl$_3$ suggesting coordination to Al^{3+}. This supports the observation of the tetrahedrally and octahedrally coordinated Al-[Tf$_2$N] species assigned in the ^{27}Al spectra (Fig. 6). A similar upfield shift in the nitrogen peak for the [Tf$_2$N]$^-$ anion is not seen in the spectrum of the [C$_2$TMEDA][Tf$_2$N] mixture.

^{19}F spectra of {AlCl$_3$ +.[C$_4$mpyr][Tf$_2$N]} are given in Fig. 8. Like the ^{27}Al spectra, the ^{19}F spectra also suggest the presence of complexes of Al with Cl$^-$ and [Tf$_2$N]$^-$ anions. The large singlet at - 80.8 ppm (298 K) in Fig. 8 can be attributed to the free [Tf$_2$N]$^-$ anions (see Castiglioni et al.[44]) whereas the underlying multiplet signals in the range (-77 - -81.5) ppm (at 298 K) are probably the mixed (AlCl$_x$[Tf$_2$N]$_{(4-x)}$)$^-$ complex anions. ^{19}F NMR spectra for dilute CDCl$_3$ and CD$_2$Cl$_2$ solutions of Al ion complexes with [Tf$_2$N]$^-$ anions show complex multiplets.[8] The main peak in Fig. 8 broadens and moves downfield with increasing temperature.

Density.

There are very few volumetric studies of AlCl$_3$ solutions in molten salts or ionic liquids that might be compared to the systems studied here. The limiting apparent molar volume of AlCl$_3$ in the room-temperature ionic liquid 1-ethyl-3-
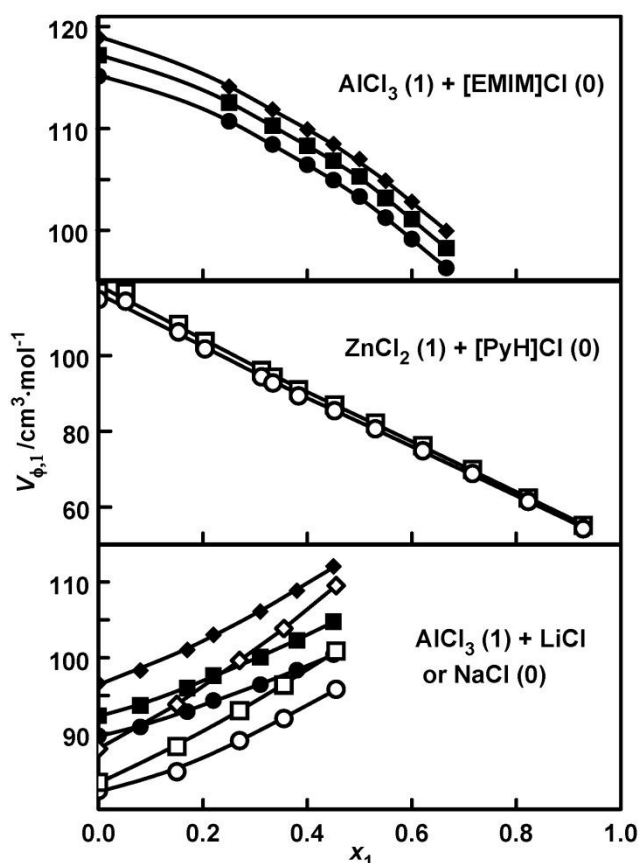
Fig. 9. Apparent molar volumes ($V_{\phi,1}$) of AlCl$_3$ in [EMIM]Cl, of ZnCl$_2$ in [PyrH]Cl, and of AlCl$_3$ in LiCl and NaCl, calculated from the data of ref. 45, 46 and 47 respectively, as a function of solute mole fraction, x_1. Symbols: upper panel, ●, 303 K; ■, 333 K; ◆, 358 K; central panel, ○, 420 K; □, 460 K; lower panel, AlCl$_3$ in LiCl, ●, 900 K; ■, 1000 K; ◆, 1050 K; AlCl$_3$ in NaCl, ○, 900 K; □, 1000 K; ◇, 1050 K. The linearity of the ZnCl$_2$ plot is of interest given that the phase diagram of this system shows compound formation at x = 0.33, 0.5 and 0.66.[46]
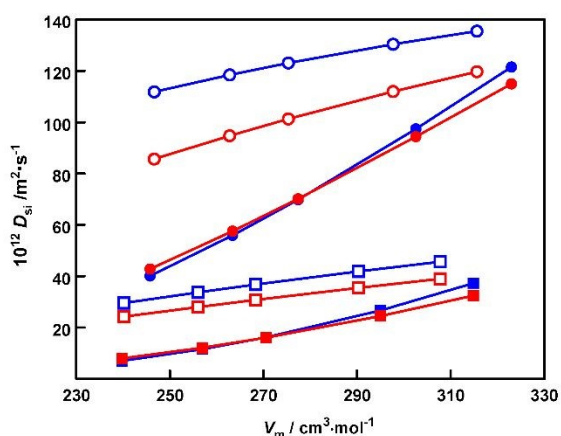

Fig. 10. Comparison of the molar volume dependence of the intra-diffusion coefficients of the cation and anion in {AlCl$_3$ + [C$_2$TMEDA][Tf$_2$N]} and {AlCl$_3$ + [C$_4$mpyr][Tf$_2$N]} at 323.15 and 363.15 K. Symbols: cations, blue; anions, red; 323.15 K, squares; 363.15 K, circles; [C$_2$TMEDA][Tf$_2$N], solid; [C$_4$mpyr][Tf$_2$N], open. The D(Al species) values in {AlCl$_3$ + [C$_4$mpyr][Tf$_2$N]} at 323.15 K overlap those of the anion and are not shown.

methylimidazolium chloride, [EMIM]Cl, calculated from the density data of Fannin et al.,[45] varies from 115 to 118 cm$^3 \cdot$mol^{-1} between (303 and 353) K. In this system, $V_{\phi,1}$ decreases with increasing AlCl$_3$ content, by about 7% to mole fraction 0.33. In the mixtures of ZnCl$_2$ with pyridinium chloride, [PyH]Cl, calculated from the density data of Easteal and Angell,[46] again $V_{\phi,1}$ decreases with increasing salt content (Fig. 10). This is also the case for the system {Li[FSI] + [C$_3$mpyr][FSI]},[34] so this appears to be common behaviour. On the other hand, in the high-temperature molten salts LiCl and NaCl, the limiting apparent molar volume of AlCl$_3$, calculated from the density data of Sato et al.,[47] has the much smaller values 89 and 80 cm$^3 \cdot$mol^{-1} respectively at 1173 K, and $V_{\phi,1}$ increases with increasing AlCl$_3$ content, by about 18% to mole fraction 0.33, presumably due to the formation of the species [AlCl$_4$]$^-$.[48,49] So there is considerable variation in both the magnitude and composition dependence of $V_{\phi,1}(m)$, depending on the system.

In the two cases examined here, $V_{\phi,1}^0$ for AlCl$_3$ at infinite dilution is smaller in [C$_2$TMEDA][Tf$_2$N], at approximately 62 cm^{3}mol^{-1} at 298.15 K, than in [C$_4$mpyr][Tf$_2$N], at 81 cm$^3 \cdot$mol^{-1} at the same temperature (Fig. 2). The latter value is close to the molar volume of pure AlCl$_3$ (80 cm$^3 \cdot$mol^{-1}), were it liquid at room temperature, estimated by extrapolation of the high temperature density measurements of Sato et al.[50] However Fig. 9 shows $V_{\phi,1}^\infty$ can vary considerably from one system to another as well as with temperature.

The AlCl$_3$ species do not interact at infinite dilution, so this difference in $V_{\phi,1}^\infty$ reflects a difference in the ionic liquid – solute interactions, the AlCl$_3$ packing more efficiently in [C$_2$TMEDA][Tf$_2$N] than in [C$_4$mpyr][Tf$_2$N]. The molar volumes of the two ionic liquids differ by only 2%, so this may be due to the chain structure of the [C$_2$TMEDA]$^+$ cation as the solute-anion interactions must be the same in the two ionic liquids.

The second difference between the two systems is the increase in apparent molar volume with increasing AlCl$_3$ concentration for the [C$_2$TMEDA][Tf$_2$N] system and the corresponding decrease for the [C$_4$mpyr][Tf$_2$N] system, though the changes are not large. The composition dependence of the volumes is stronger in both systems (Fig. 3), the limiting values at each temperature of course being identical ($V_{\phi,1}^0 = V_1^0$).

Complexation of AlCl$_3$ with the [Tf$_2$N]$^-$ ion has been reported for solutions in [BMP][Tf$_2$N] (= [C$_4$mpyr][Tf$_2$N]) and [EMIM][Tf$_2$N][§§] at similar concentrations based on ^{19}F and ^{27}Al NMR and Raman spectroscopy and in [C$_3$mpip][Tf$_2$N] and [C$_4$mpyr][Tf$_2$N] based on ^{27}Al NMR measurements[9] respectively. If similar complexation occurs in [C$_2$TMEDA][Tf$_2$N] and [C$_4$mpyr][Tf$_2$N], having the same anion, the different limiting values and composition dependence must be due to interactions of the different cations with the complexed anions. This is consistent with the cation-AlCl$_3$ interaction detected in the ^{15}N and ^{27}Al NMR spectra for the [C$_2$TMEDA][Tf$_2$N] mixtures.

It should be noted that the molar volume [$V_m \equiv V/(n_0+n_1)$] of both solutions decreases with increasing AlCl$_3$ concentration as the smaller AlCl$_3$ replaces the larger ionic liquid ions. As the densities and molar masses are similar, the molar volumes are also similar (see below).
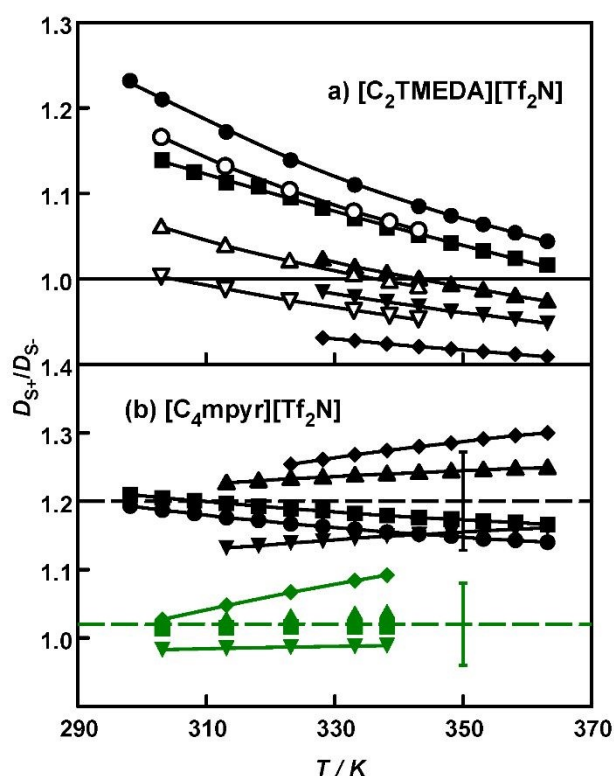
Fig. 11. (a) Intra-diffusion coefficient ratios (D_{s+}/D_{s-}) for [C$_2$TMEDA][Tf$_2$N] and its mixtures with AlCl$_3$, as a function of temperature. Note that the ratio for the ionic liquid [C$_2$dmppz][Tf$_2$N], with the closed-ring analogue cation of [C$_2$TMEDA]$^+$, is (1.27 ± 0.01), independent of temperature. [1] (b) Intra-diffusion coefficient ratios (D_{s+}/D_{s-}) and (D_s(Al species)/ D_{s-}) for [C$_4$mpyr][Tf$_2$N] and its mixtures with AlCl$_3$ (green symbols) as a function of temperature. Note that the first ratio is constant (1.20 ± 0.03) and the second is essentially unity, within the combined experimental uncertainties (6%). Symbols: ●, m_1 = 0 mol·kg^{-1}; ○, 0.016 mol·kg^{-1}; ■, m_1 = 0.2 mol·kg^{-1}; ▲, m_1 = 0.5 mol·kg^{-1}; △, 0.56 mol·kg^{-1}; ▽, 0.8 mol·kg^{-1}; ◆, m_1 = 1.0 mol·kg^{-1}.

Intra-diffusion.

At first sight, the two systems show quite different diffusive behaviour. Fig. 10 shows the dependence of the intra-diffusion coefficients on solution molar volume at two temperatures, 323 K and 363 K, as examples. The [C$_4$mpyr][Tf$_2$N] system has higher intra-diffusion coefficients, with a clear difference between cation and anion, the former being the larger, with a linear molar volume dependence (at these temperatures), whereas the [C$_2$TMEDA][Tf$_2$N] system has lower intra-diffusion coefficients, with similar values for the two ions, and a clear non-linear volume dependence.

In common with intra-diffusion in many pure ionic liquids,[‡,12,13,20,22-24,51,52,] the ratio of the cation and anion intra-diffusion coefficients (calculated from the Litovitz equations for each composition) shows very little temperature dependence in the case of {AlCl$_3$ + [C$_4$mpyr][Tf$_2$N]}, having an average of (1.20 ± 0.03) for both the pure ionic liquid and the mixtures (Fig. 10).

A similar result applies to the ratios of the intra-diffusion coefficient of the tetrahedrally coordinated Al-containing

species (probably [AlCl$_4$]$^-$, see above) to those of the ionic liquid cation and anion: curiously, the latter ratio is unity within the experimental uncertainty (1.00 ± 0.03) in the temperature range of the Al intra-diffusion measurements (303- 338 K). This suggests that diffusion of both the anion and the Al-species is controlled by fluctuations in the number density of surrounding cations – essentially a caging effect. The ^{27}Al spectra show relatively low concentrations of [Tf$_2$N]$^-$ complexes as mentioned above, so one cannot explain this effect in terms of AlCl$_3$-anion ion association.

On the other hand, the ratio of the cation and anion intra-diffusion coefficients for {AlCl$_3$ + [C$_2$TMEDA][Tf$_2$N]}, like that of the pure ionic liquid, is strongly temperature dependent, decreasing with increasing temperature. For the mixtures it is also strongly composition dependent, so that at high concentrations and temperatures, the anion diffuses more quickly than the cation (Fig. 11). In this case, the single Al-species intra-diffusion coefficient we were able to measure is 0.88 of that for the anion at the same composition and temperature [0.16 mol·kg^{-1}, 338 K; calculated from eqn 16]. This is again more consistent with caging rather than AlCl$_3$-[Tf$_2$N]$^-$ association.

Free volume theories have been applied to the transport properties of liquids in various versions for many years.[17,18,25,53,54,55] The central postulate is that particle movement is governed by changes in volume with temperature and composition, relative to a close packed phase, solid or glass. The majority of these are empirical or semiempirical, but Liu has recently put the theory on a sounder basis, obtaining power-law free volume expressions for the intra-diffusion coefficient, viscosity and thermal conductivity of the hard sphere fluid and fitting these to what are now well-established and reliable values obtained from molecular dynamics simulations.[19] In doing so he has confirmed the validity of the power-law form of the empirical Ertl-Dullien free-volume expression[17,18]
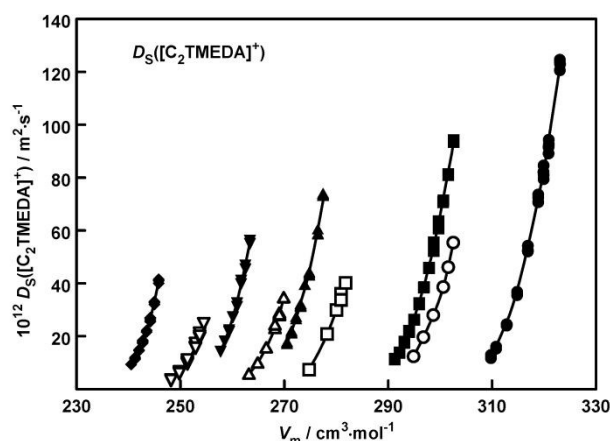

Fig. 12. Experimental intra-diffusion coefficients of the [C$_2$TMEDA]+ ion in {AlCl$_3$ + [C$_2$TMEDA][Tf$_2$N]} mixtures plotted against the mixture molar volumes. Symbols: steady gradient measurements (UNSW), ●, m1 = 0 mol·kg^{-1}; ■, m1 = 0.2 mol·kg^{-1}; ▲, m1 = 0.5 mol·kg^{-1}; ◆, m1 = 1.0 mol·kg^{-1}; PGSE measurements (WSU), ○, 0.016 mol·kg^{-1}; □, 0.4 mol·kg^{-1}; △, 0.56 mol·kg^{-1}; ▽, 0.8 mol·kg^{-1}.

ARTICLE

<div align="right">Journal Name</div>

Table 6. Coefficients of eqn 18 for the systems {AlCl₃ + [C₂TMEDA][Tf₂N]}, {AlCl₃ + [C₄mpyr][Tf₂N]} and {Li[FSI] + [C₃mpyr][FSI]}

	{AlCl$_3$ + [C$_2$TMEDA][Tf$_2$N]},		{AlCl$_3$ + [C$_4$mpyr][Tf$_2$N]}			{Li[FSI] + [C$_3$mpyr][FSI]}		
	D_{s+}	D_{s-}	D_{s+}	D_{s-}	D(Al species)	D_{s+}	D_{s-}	D_s(Li$^+$) ^{a}
ln(B/10^{-12} m^2·s^{-1})	13.23 ± 0.13	13.79 ± 0.17	12.31 ± 0.16	11.95 ± 0.33	12.64 ± 0.61	11.77 ± 0.17	12.12 ± 0.21	11.88 ± 0.26
n	3.583 ± 0.077	3.846 ± 0.099	3.014 ± 0.089	2.90 ± 0.18	3.26 ± 0.33	2.840 ± 0.090	3.01 ± 0.12	3.04 ± 0.14
V_g/ cm³·	294.90 ± 0.38	294.71 ± 0.48	290.44 ± 0.48	291.04 ± 1.0	288.8 ± 1.6	218.65 ± 0.35	217.33 ± 0.47	217.35 ± 0.57
c/kg·	0.314 32 ± 0.000 45	0.317 70 ± 0.000 53	0.298 72 ± 0.000 39	0.298 98 ± 0.000 78	0.278 26 ± 0.000 86	0.0994 ± 0.0022	0.0938 ± 0.0028	0.0720 ± 0.0032
d/ kg²·mol^{-2}	-0.032 49 ± 0.000 43	-0.031 16 ± 0.000 51	-0.026 76 ± 0.000 41	-0.028 68 ± 0.000 79	-0.066 30 ± 0.000 71	0.2443 ± 0.0072	0.2487 ± 0.0090	0.3210 ± 0.0099
e/ kg³·mol^{-3}	-	-	-	-	-	-0.1859 ± 0.0051	-0.1876 ± 0.0065	-0.2368 ± 0.0071
st. devn of fit /%	3.1	3.7	2.6	3.7	2.5	2.5	3.0	3.0
T range/K	298-363		298-363		303-338	273-353		
m_{max}/mol·kg^{-1}	1		1			1		
x_{max}	0.3		0.3			0.23		

^{a} It was necessary to include extrapolated values for m = 0 mol·kg^{-1} to best fit the Li$^+$ intra-diffusion data. These are listed in Table 6 of ref. 34.

Table 7. Mean volume offsets (V_m^{offset}) for the systems {AlCl₃ + [C₂TMEDA][Tf₂N]}, {AlCl₃ + [C₄mpyr][Tf₂N]} and {Li[FSI] + [C₃mpyr][FSI]}. ^{a,b}

	{AlCl$_3$ + [C$_2$TMEDA][Tf$_2$N]}		{AlCl$_3$ + [C$_4$mpyr][Tf$_2$N]}				{Li[FSI] + [C$_3$mpyr][FSI]}		
m/mol·kg^{-1}	cation	anion	m/mol·kg^{-1}	cation	anion	Al species	m/mol·kg^{-1}	cation	anion	Li$^+$ ^{c}
0.1607	14.86 ± 0.15	14.93 ± 0.06	0.1995	17.08 ± 0.21	17.09 ± 0.24	17.12 ± 0.15	0.32	11.13 ± 0.17	10.83 ± 0.17	10.57 ± 0.17
0.2005	18.32 ± 0.22	18.59 ± 0.14	0.5003	38.56 ± 0.48	38.57 ± 0.35	38.53 ± 0.34	0.4811	17.80 ± 0.27	17.40 ± 0.26	17.57 ± 0.27
0.3994	33.63 ± 0.31	34.17 ^{c}	0.6997	50.35 ± 0.65	50.35 ± 0.59	50.40 ± 0.45	0.9622	30.97 ± 0.47	30.41 ± 0.46	30.83 ± 0.46
0.5034	41.05 ± 0.34	41.70 ± 0.26	1.0001	65.77 ± 0.82	65.76 ± 0.62	65.53 ± 0.60				
0.5587	44.27 ± 0.37	44.95 ± 0.15								
0.7027	53.40 ± 0.31	54.19 ± 0.28								
0.7950	57.71 ± 0.48	58.46 ± 0.45								
1.0038	68.85 ± 0.48	69.89 ± 0.36								

^{a} The uncertainties given for the offset volumes are standard deviations. The units are cm³·mol^{-1}. ^{b} The mean offsets increase slightly with increasing temperature, more so at the higher compositions, *e.g.* from 69.08 cm³·mol^{-1} at 328 K to 70.60 cm³·mol^{-1}·at 363 K for the anion in {AlCl₃ + [C₂TMEDA][Tf₂N]} at m = 1 mol·kg^{-1}. This secondary effect has not been included in eq (18) as the precision of the data is not sufficient to warrant inclusion of an arbitrary temperature dependence. Fitting ($D_S/\sqrt{T}$), for example, does not improve the goodness of fit or remove this temperature effect, as the parameters n, c, d and e hardly change. We note Liu[19] scaled reduced intra-diffusion coefficients for the Lennard-Jones fluid onto data for the hard-sphere fluid with an exponential temperature factor, exp(-constant/T^*), but there the available reduced temperature range, ($T^* =k_BT/\varepsilon$), is quite large, with 0.9 < T^* < 10. ^{c} It was necessary to include extrapolated values for m = 0 mol·kg^{-1}. to best fit the Li$^+$ intra-diffusion data (see Table 6). These are listed in Table 6 of ref. 34. ^{d} There is only one datum for this composition
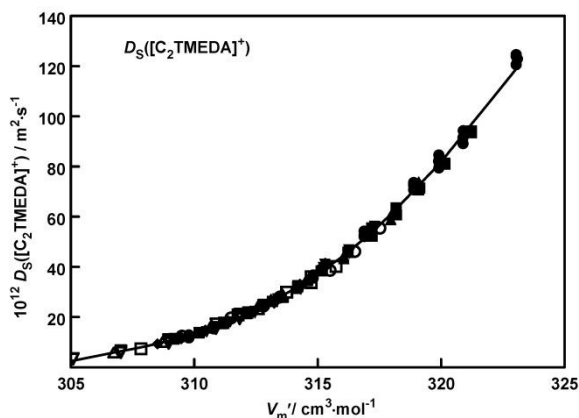
Journal Name

ARTICLE

Fig. 13. Experimental intra-diffusion coefficients of the $[C_2TMEDA]^+$ ion in {AlCl$_3$ + [C$_2$TMEDA][Tf$_2$N]} mixtures fitted to eqn. 18. $V_m'=V_m(1+cm+dm^2+em^3)$.

$$D_{si} = B[(V_m - V_g)/V_g]^n \qquad (17)$$

where the free volume V_f is defined as $(V_m - V_g)$. This can be regarded as the difference between the volume of the liquid and that of a close-packed phase at which diffusion is infinitely slow, at the simplest level with n = 1.[56,57] For the hard sphere fluid, using reduced intra-diffusion coefficients,‡‡ Liu's analysis yields n = 0.74:[19] However, real fluids are best fit with $n > 1$.[17,18] Here the Ertl-Dullien approach is extended to the AlCl$_3$ ionic liquid mixtures.

Fig. 12 shows a plot of the experimental intra-diffusion coefficients of the $[C_2TMEDA]^+$ ion in the {AlCl$_3$ + [C$_2$TMEDA][Tf$_2$N]} mixtures against the molar volume. The iso-concentration curves are found to have a very similar (in the geometric sense) volume dependence when fitted to eqn 17, that is, the parameters B and n were similar, with V_0 decreasing with increasing molality, consistent with trends shown in Fig. 12. The same result is found for the anion in this system and the three ions in the {AlCl$_3$ + [C$_4$mpyr][Tf$_2$N]} mixtures. This suggests that for a given ion, the iso-concentration lines can be superposed,

$$D_{si}(T,m) = B\{V_m(T,m)[1+cm+dm^2+em^3]/V_g^\infty -1\}^n \quad (18)$$

where V_g^∞ is V_g at infinite dilution, that is at m = 0 mol·kg^{-1}. The concentration dependent offset is

$$V_m^{offset} = V_m(T,m)[1+cm+dm^2+em^3]-V_m(T,m)$$
$$= V_m(T,m)[cm+dm^2+em^3] \qquad (19)$$

This is illustrated in Fig. 13. The free volume at each state point is then given by

$$V_f(T,m) = V_m(T,m) - V_g(m) \qquad (20)$$
$$= V_m(T,m) - V_g^\infty /(1+cm+dm^2+em^3)$$

The separation of the temperature dependence of V_m from its composition dependence was originally suggested by Cullinan[58] for organic liquid mixtures: however, our approach differs in its practical application. Expressing the fit in terms of the molality is superior to using the mole fraction, where more terms are required and are of similar magnitude, that is, convergence is slow. Nevertheless, as should be expected, the offset volumes are the same using either concentration scale. Table 6 lists the coefficients of eqn 18 for the intra-diffusion coefficients obtained using a nonlinear least-squares regression (Mathsoft Axum 5.0 graphics software). It also includes parameters for the ionic liquid mixture {Li[Tf$_2$N] + [C$_3$mpyr][FSI]} for comparison, using data from previous work (3 compositions, including the solvent ionic liquid)[34] together with those of Hayamizu et al. (1 composition)[59]. Table 7 lists the volume offsets.

The fits show remarkable agreement for the offset volumes for each system, particularly for the anion and cation. There is also good agreement for V_o and n for each of the {AlCl$_3$ + [C$_4$mpyr][Tf$_2$N]}and {Li[Tf$_2$N] + [C$_3$mpyr][FSI]} mixtures. The differences observed for {AlCl$_3$ + [C$_2$TMEDA][Tf$_2$N]} mixtures reflect the difference in the temperature dependence of the intra-diffusion coefficients for the cation and anion in this system remarked upon above.

These observations are consistent with a common free volume dependence for each species in a particular mixture at a given composition, within the composition range studied. In the case of the {AlCl$_3$ + [C$_4$mpyr][Tf$_2$N]} system, this approaches the point where it separates into two phases ($x \approx 0.33$).[9] It seems that from the viewpoint of ion transport the solutions, in effect, retain the basic structure of the neat ionic liquid solvent, with diffusion depending on an effective molar volume, as shown in Fig. 13. Thus the intra-diffusion process depends on separable density (V_0) and thermodynamic terms (the offset), the latter being primarily a dilution effect as solute species replace solvent species (*c.f.* Raoult's law). The former reflects the typical dependence of liquid transport properties on the repulsive forces, with the second being moderated by the attractive forces. Complexation of AlCl$_3$ by the [Tf$_2$N]$^-$ or $[C_2TMEDA]^+$ ions seems to play little part in the transport of mass and charge in these two systems.

Conclusions

Densities and intra-diffusion coefficients have been determined for the systems {AlCl$_3$ + [C$_2$TMEDA][Tf$_2$N]} and {AlCl$_3$ + [C$_4$mpyr][Tf$_2$N]} over a range of temperatures between 298 and 363 K, depending on the concentration and competing T_2 relaxation, up to concentrations of AlCl$_3$ of 1 mol·kg^{-1}. For intra-

ARTICLE

Journal Name

diffusion, both pulsed and steady gradient spin-echo NMR has been employed for the cation and anion coefficients for the first system and for cations in the second, with good agreement between the two methods. Intra-diffusion of the of the Al species in the second system was determined by the pulsed gradient method at temperatures between 303 and 338 K, the upper limit being the point at which convection affected measurements. Shorter T_2 relaxation times in {AlCl$_3$ + [C$_2$TMEDA][Tf$_2$N]} mixtures prevented measurements in this system except at the lowest composition, 0.16 mol·kg^{-1}, and the highest temperature, 338 K.

^{27}Al, ^{15}N and ^{19}F NMR spectroscopy has been used to examine interactions in the AlCl$_3$-ionic liquid mixtures.

The two systems show different behaviour when the density and intra-diffusion coefficient data are analysed.

The expansivities, [α_p = -($\partial\rho/\partial T)_p/\rho$], calculated from the densities increase with m for [C$_4$mpyr][Tf$_2$N] mixtures, but decrease for [C$_2$TMEDA][Tf$_2$N] mixtures. The apparent molar and   volumes increase with increasing [AlCl$_3$] for the [C$_2$TMEDA][Tf$_2$N] system but decrease for the [C$_4$mpyr][Tf$_2$N] system. There appears to be a cation effect even if the anion complexes with AlCl$_3$, as the apparent molar volume at infinite dilution, $V_{\phi,1}^{\infty}$, is much smaller in [C$_2$TMEDA][Tf$_2$N] than in [C$_4$mpyr][Tf$_2$N] at the same temperature and this is attributed to complexation between AlCl$_3$ and the [C$_2$TMEDA] ion deduced from ^{15}N and ^{27}Al NMR, leading to more efficient packing. It seems however that cation complexation leads to higher apparent molar volumes at higher concentration whereas anion complexation has the opposite effect.

In the {AlCl$_3$ + [C$_2$TMEDA][Tf$_2$N]} mixtures the ionic liquid ion intra-diffusion coefficients differ in their temperature dependence such that at lower concentrations and temperatures, the anion diffuses more quickly than the cation, whereas at higher concentrations and temperatures the reverse is true. In {AlCl$_3$ + [C$_4$mpyr][Tf$_2$N]} mixtures the ratio of the cation and anion intra-diffusion coefficients is a constant, 1.20 ±0.03, independent of temperature and composition. The ratio of the intra-diffusion coefficient of the Al species to that of the anion is unity, again independent of temperature and composition. For the {AlCl$_3$ + [C$_2$TMEDA][Tf$_2$N]} mixture, this ratio was 0.88 for the single state point measurable. This suggests that diffusion of both the anion and the Al-species in both systems is controlled by fluctuations in the density of surrounding cations – essentially a caging effect. The intra-diffusion coefficients show a Litovitz temperature dependence at all compositions and an exponential dependence on the molality.

The major finding of this work comes from the application of the Ertl-Dullien free volume expression for the intra-diffusion coefficients to these systems. Iso-concentration lines for a given species form geometrically similar curves when plotted against molar volume (that is, the power law exponent is the same at each composition) and can be mapped onto the line for the pure ionic liquid by appropriate volume shifts. Therefore the temperature dependence of the free volume is independent of composition, whatever the speciation of the AlCl$_3$-[Tf$_2$N]$^-$ complexes that might be formed, or the interaction between

AlCl$_3$ and the [C$_2$TMEDA]$^+$ ion, demonstrated by the NMR spectra. It also shows that the intra-diffusion process depends on separable density (V_0) and thermodynamic terms (the free volume offset), the latter being primarily a colligative, dilution effect as solute species replace solvent species. The former reflects the typical dependence of liquid transport properties on the repulsive forces, with the second being moderated by the attractive forces. These results suggest that the application of free volume theories might be fruitful in the study of the transport properties of ionic liquid solutions and mixtures.

Appendix

Laity[60,61] used Onsager non-equilibrium thermodynamics[62] to define resistance coefficients (r_{ij}, i,j = +,-) for molten salts. These are a generalisation of the Stokes-Einstein-Sutherland frictional coefficient for tracer diffusion in a solvent continuum. He suggested that negative like-ion resistance coefficients might indicate ion-ion association in one component molten salts on the basis of the known ion association in molten ZnCl$_2$. Subsequently, Harris examined a number of examples using data that had become available since Laity's work and confirmed Laity's suggestion by treating weakly ionised liquids such as water and molecular acids with his methods.[63] Calculation of resistance coefficients for numerous ionic liquid examples since has shown they are almost always positive,[16,23,24,64,65,66] with very few exceptions.[67,68] This is consistent with Nernst-Einstein deviation parameters, Δ, lying in the range $0 < \Delta < 0.5$, as they do for simple unassociated high-temperature molten salts.[63,69,70,71] For associated salts, with both like-ion resistance coefficients, r_{ii}, being negative, $0.5 < \Delta < 1$.[63,68]

The requisite arguments and equations are given in detail in ref. 20 and 60. As our work on [C$_4$mpyr][Tf$_2$N], [C$_2$dmppz][Tf$_2$N], and [C$_2$TMEDA][Tf$_2$N] was published prior to these papers, resistance coefficients were not calculated at that time, only velocity cross-correlation coefficients and Nernst-Einstein deviation parameters. Table S7 in the ESI† lists the actual values – both like ion are positive - and the viscosity dependence is
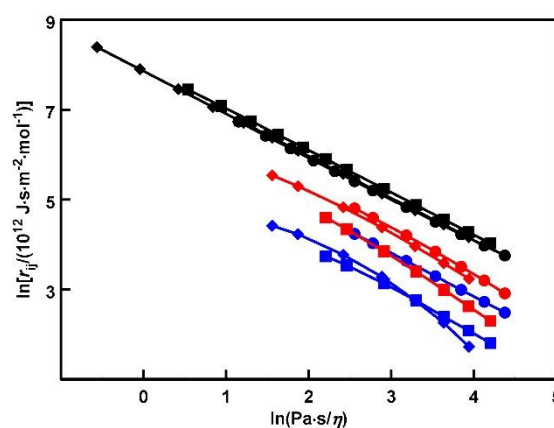

Fig. 14. Laity Resistance coefficients, r_{ij}, for [C$_4$mpyr][Tf$_2$N], [C$_2$TMEDA][Tf$_2$N] and [C$_2$dmppz][Tf$_2$N]. Symbols: black, r_{+-}, (cation-anion); blue, r_{++},(cation-cation); red, r_{--}, (anion-anion); ●, [C$_4$mpyr][Tf$_2$N]; ■, [C$_2$TMEDA][Tf$_2$N]; ◆, [C$_2$dmppz][Tf$_2$N].

shown in Fig. 14. Note that for each substance, at a given viscosity, $r_{+-} > r_{--} > r_{++}$ for these salts, that is, the resistance coefficient is largest for the cation-anion interaction, as is always the case, and is smallest for the cation-cation interaction. Resistance coefficients have the advantage that they do not depend on the choice of particle velocity reference frame, even in multicomponent systems. The linearity of the r_{+-} isobars is a variant of the (fractional) Walden relation, as r_{+-} is inversely proportional to the molar conductivity.[9,10]

Author Contributions

K. R. Harris: conceptualization, formal analysis, investigation (intra-diffusion measurements by steady gradient spin-echo NMR; density measurements and analysis), resources, methodology, validation, writing - original draft, writing - review & editing, visualisation. N. Kanai: investigation (intra-diffusion measurements for the $AlCl_3$ species in the [C_4mpyr][Tf_2N] mixtures by PGSTE and DSTE spin-echo NMR), writing - review & editing. W. S. Price: resources, methodology, supervision, writing − review and editing. T. Rodopoulos: resources, supervision, writing - original draft, writing - review & editing. T. Rüther: conceptualization, resources, investigation (sample preparation), writing - review & editing. A. M. Torres: investigation (intra-diffusion measurements for the $AlCl_3$ species in the [C_2TMEDA][Tf_2N] mixtures by PGSTE and DSTE spin-echo NMR), writing - review & editing. J.-P Veder: investigation (sample preparation, ^{15}N NMR spectroscopy). S. A. Willis: investigation (assistance with NMR experiments and analysis at WSU), resources, writing − review & editing.

Conflicts of interest

There are no conflicts to declare.

Acknowledgements

Notes and references

‡ The abbreviation [Pyr_{14}][Tf_2N] is also used in the literature.

§ Intra-diffusion is defined as the interdiffusion of distinguishable but otherwise physically and chemically identical ions or molecules in a multi-component system (ref. 14 and 15). The term self-diffusion is often employed in the literature, but this is better reserved for single component systems such as an undiluted ionic liquid. However, the symbol D_S is used for both quantities as D_I could be confused with the so-called "intrinsic" diffusion coefficient (ref. 25, p. 72 ff), a quantity ill-defined in fluid systems, and best avoided.

§§ [BMP]$^+$ and [C_4mpyr]$^+$ = 1-butyl-1-methylpyrrolidinium; [C_3mpip]$^+$ = 1-propyl-1-methylpiperidinium; [EMIM]$^+$ = 1-ethyl-3-methylimidazolium.

‡ 1-Alkyl-3-methylimidazolium salts: [HMIM][PF_6], [OMIM][PF_6], [HMIM][BF_4], [OMIM][BF_4], [BMIM][Tf_2N], [OMIM][Tf_2N]; pyrrolidinium salts: [Pyr_{13}][FSI], [Pyr_{14}][Tf_2N]; ammonium salts: [N_{1125}][Tf_2N], [N_{1127}][Tf_2N], [$N_{112,2}O_2O_1$][Tf_2N], [$N_{112,2}OCO_1$][Tf_2N]; others: [EMIM][TCB], [EMIM][CF_3SO_3], [choline][Tf_2N] and [3-ABN_{13}][Tf_2N]. Exceptions: [BMIM][PF_6], [OMIM][BF_4], [EMIM][Tf_2N] and [HMIM][Tf_2N] and, very probably, [EMIM][CH_3SO_3] and [EMIM][FAP], where data from other sources were combined with our own.

‡‡ The use of the reduced self-diffusion coefficient ($D*$) introduces a basic $\sqrt{T}$ temperature dependence deriving from the Chapman-Enskog expression for the hard sphere dilute gas self-diffusion coefficient:

$$D* = D / D_0 g(\sigma); \quad D_0 = (3/8\rho\sigma^2)\sqrt{(kT/\pi m)}$$

$g(\sigma)$ being the radial distribution function at contact, ρ the density, σ the sphere diameter and m its mass. As Liu points out, this suggests the constant B might be proportional to $\sqrt{T}$. Inclusion of a $\sqrt{T}$ factor in eqn 18, worsens the fits, especially at the higher temperatures: hence we have used the original Ertl-Dullien form of the free-volume expression for D_s.

1 A. P. Abbott and K. J. McKenzie, *Phys. Chem. Chem. Phys.*, 2006, **8**, 4265–4279.

2 Y. Melamed, N. Maity, L. Meshi and N. Eliaz, *Coatings,* 2021, **11**, 1414.

3 G. Saevarsdottir, H. Kvande, B. J. Welch, *JOM,* 2020, **72**, 296–308.

4 Y. Zhao and T. J. VanderNoot, *Electrochim. Acta*, 1997, **42**, 3 – 13.

5 K. K. Maniam and S. Paul, *Coatings*, 2021, **11**, 80.

6 S. Zein El Abedin, E. M. Moustafa, R. Hempelmann, H. Natter and F. Endres, *Electrochem. Commun.*, 2005, **7**, 1111 – 1116.

7 S. Zein El Abedin, E. M. Moustafa, R. Hempelmann, H. Natter and F. Endres, *ChemPhysChem*, 2006, **7**, 1535 – 1543.

8 N. M. Rocher, E. I. Izgorodina, T. Rüther, M. Forsyth, D. R. MacFarlane; T. Rodopoulos; M. D. Horne and A. M. Bond, *Chem. Eur. J.,* 2009, **15**, 3435-3447.

9 T. Rodopoulos, L. Smith, M. D. Horne and T. Rüther, *Chem. Eur. J.,* 2010, **16**, 3815-3826.

10 T. Rodopoulos, M. D. Horne and T. Rüther, Electrorecovery of Metals, PCT Int. Appl., 2010, WO 2010105299 A1 20100923.

11 J.-P. Veder, M. D. Horne, T. Rüther, A. M. Bond and T. Rodopoulos, *Electrochem. Comm.*, 2013, **37**, 68-70.

12 T. Rüther, K. R. Harris, M. D. Horne, M. Kanakubo, T. Rodopoulos, J.-P. Veder and L. A. Woolf, *Chem. Eur. J.,* 2013, **19**, 17733-17744.

13 K. R. Harris, L. A. Woolf, M. Kanakubo and T. Rüther, *J. Chem.*

Eng. Data, 2011, **56**, 4672-4685.

14   H. J. V. Tyrrell and K. R. Harris, *Diffusion in Liquids*, Butterworths, London, 1984, p. 4.

15   J. G. Albright and R. Mills, *J. Phys. Chem*., 1965, **69**, 3120-3126.

16   K. R. Harris and M. Kanakubo, *Phys. Chem. Chem. Phys*., 2022, **24**, 14430–14439.

17   H. Ertl and F. A. L. Dullien, *A.I.Ch.E. J*., 1973, **19**, 1215–1223.

18   H. Ertl and F. A. L. Dullien, *J. Phys. Chem.*, 1973, **77**, 3007–3011.

19   H. Liu, *J. Appl. Phys*., 2021, **129**, 044701.

20   K. R. Harris, M. Kanakubo and L. A. Woolf, *J. Chem. Eng. Data*, 2006, **51**, 1161-1167.

21   The NIST Reference on Constants, Units and Uncertainty, https://physics.nist.gov/cuu/Uncertainty/index.html, (accessed May 2022).

22   M. Kanakubo, K. R. Harris, N. Tsuchihashi, K. Ibuki and M. Ueno, *J. Phys. Chem. B*, 2007, **111**, 2062–2069.

23   K. R. Harris and M. Kanakubo, *Phys. Chem. Chem. Phys.*, 2015, **17**, 23977-23993.

24   K. R. Harris and M. Kanakubo, *J. Phys. Chem. B*, 2016, **120**, 12937–12949.

25   H. J. V. Tyrrell and K. R. Harris, *Diffusion in Liquids*, Butterworths, London, 1984; p. 225.

26   J. E. Tanner, *J. Chem. Phys.*, 1970, **52**, 2523-2526.

27   A. Jerschow and N. Müller, *J. Magn. Reson.*, 1997, **125**, 372-375.

28   W. S. Price and P. W. Kuchel, *J. Magn. Reson.*, 1991, **94**, 133-139.

29   W. S. Price, *Concepts Magn. Reson*., 1997, **9**, 299-336.

30   W. S. Price, *Concepts Magn. Reson.,* 1998, **10**, 197-237.

31   E. O. Stejskal and J. E. Tanner, *J. Chem. Phys.*, 1965, **42**, 288-292.

32   L. G. Longsworth, *J. Phys. Chem*., 1960, **64**, 1914-1917.

33   R. Mills, *J. Phys. Chem*., 1973, **77**, 685-688.

34   T. Rüther, M. Kanakubo, A. S. Best and K. R. Harris, *Phys. Chem. Chem. Phys*., 2017, **19**, 10527-10542.

35   H. D. Ellerton, G. Reinfelds, D. E. Mulcahy and P. J. Dunlop, *J. Phys. Chem*., 1964, **68**, 398-402.

36   W. Geffcken, *Z. physik. Chem*., 1931, **A155**, 1-28.

37   G. D. Zissi and C. Bessada, *Z. Naturforsch*., *A: Phys. Sci.,* 2001, **56**, 697-701.

38   A. L. L. East and J. Hafner, *J. Phys. Chem. B*, 2007, **111**, 5316-5321.

39   C. Ferrara, V. Dall'Asta, V. Berbenni, E. Quatarone and P. Mustarelli, *J. Phys. Chem. C*, 2017, **121**, 26607-26614.

40   Y. Fang, K. Yoshii, X. Jiang, X.-G. Sun, T. Tsuda, N. Mehio and S. Dai, *Electrochim. Acta*, 2015, **100**, 82-88.

41   G. Zhu, M. Angell, C.-J. Pan, M.-C. Lin, H. Chen, C.-J. Huang, J. Lin, A. J. Achazi, P. Kaghazchi, B.-J. Hwang and H. Dai, *RSC Advances*, 2019, **9**, 11322-11330.

42   P. Eiden, Q. Liu, S. Z. El Abedin, F. Endres and I. Krossing, *Chem. Eur. J.*, 2009, **15**, 3426-3434.

43   E. I. Izgorodina, M. Forsyth and D. R. MacFarlane, *Aust. J. Chem*., 2007, **60**, 15–20.

44   F. Castiglione, M. Moreno, G. Raos, A. Famulari, A. Mele, G.B. Appetecchi and S. Passerini, S. *J. Phys. Chem. B,* 2009, **113**, 10750–10759.

45   A. A. Fannin, Jr, D. A. Floreani, L. A. King, J. S. Landers, B. J. Piersma, D. J. Stech, R. L. Vaughn, J. S. Wilkes and J. L. Williams, *J. Phys. Chem.*, 1984, **88**, 2614-2621.

46   A. J. Easteal and C. A. Angell, *J. Phys. Chem.*, 1970, **74**, 3987-3999.

47   Y. Sato, K. Kobayashi and T. Ejima, *Nippon Kinzoku Gakkaishi*, 1979, **43**, 97-104.

48   Y. Sato and T. Ejima, *Nippon Kinzoku Gakkaishi*, 1978, **42**, 905-912.

49   Y. Sato, M. Tateyama and T. Ejima, *Nippon Kinzoku Gakkaishi*, 1979, **43**, 984-991.

50   Y. Sato, M. Matsuzaki, M. Uda, A. Nagatani and T. Yamamura, *Electrochem. (Tokyo, Jpn)*, 1999, **67**, 568-572.

51   K. R. Harris, T. Makino and M. Kanakubo, *Phys. Chem. Chem. Phys.*, 2014, **16**, 9161-9170.

52   K. R. Harris and M. Kanakubo, *J. Chem. Eng. Data*, 2016, **61**, 2399-2411.

53   H. Liu, C. M. Silva and E. A. Macedo, *Fluid Phase Equilib*., 2002, **202**, 89-107.

54   O. Suárez-Iglesias, I. Medina, C. Pizarro and J. L. Bueno, *Fluid Phase Equilib*., 2008, **269**, 80-92.

55   R. V. Vaz, A. L. Magalhães, D. L. A. Fernandes and C. M. Silva, *Chem. Eng. Sci*., 2012, **79**, 153–162.

56   A. J. Batschinski, *Z. phys. Chem*., 1913, **84**, 644-706.

57   J. H. Hildebrand, *Viscosity and Diffusivity: A Predictive Treatment,* John Wiley and Sons, New York, 1977.

58   H. T. Cullinan, Jr, *Can. J. Chem. Eng.*, 1971, **49**, 130-133.

59   K. Hayamizu, S. Tsuzuki, S. Seki, K. Fujii, M. Suenaga and Y. Umebayashi, *J. Chem. Phys.*, 2010, **133**, 194505.

60   R. W. Laity, *J. Chem. Phys.* 1959, **30**, 682.

61   R. W. Laity, *Ann. N. Y. Acad. Sci.* 1960, **79**, 997.

62   L. Onsager, *Trans. N. Y. Acad. Sci.* 1945, **46**, 241.

63   K. R. Harris, *J. Phys. Chem. B*, 2016, **120**, 12135.

64   K. R. Harris and M. Kanakubo, *J. Chem. Eng. Data* 2016, **61**, 239.

65   K. R. Harris, M. Kanakubo, D. Kodama, T. Makino, Y. Mizuguchi, M. Watanabe and T. Watanabe, *J. Chem. Eng. Data*, 2018, **63**, 2015.

66 K. R. Harris and M. Kanakubo, *J. Mol. Liq.*, 2022, **358**, 119109.
67 H. Watanabe, T. Umecky, N. Arai, A. Nazet, T. Takamuku, K. R. Harris, Y. Kameda, R. Buchner and Y. Umebayashi, *J. Phys. Chem. B*, 2019, **123**, 6244.
68 K. R. Harris, *Electrochim. Acta,* 220, **337**, 135806.
69 J.-P. Hansen and I. R. McDonald, *J. Phys. C: Solid State Phys*., 1974,**7**, L384.
70 J.-P. Hansen and I. R. McDonald*, Phys. Rev. A: At., Mol., Opt. Phys.,* 1975, **11**, 2111.
71 J. Trullàs and J. A. Padró*, Phys. Rev. B: Condens. Matter Mater. Phys*. 1997, 55,12210.